

Short Note

(OC-6-35-A)-Aquadicarbonylchlorido[2-(2-pyridyl)-1,8-Naphthyridine- κ^2N^1,N^2]Ruthenium(II) Hexafluoridophosphate 2,2'-Bipyridine

Tsugiko Takase ¹, Ryosuke Abe ² and Dai Oyama ^{2,*}

¹ Institute of Environmental Radioactivity, Fukushima University, 1 Kanayagawa, Fukushima 960-1296, Japan; ttakase@sss.fukushima-u.ac.jp

² Cluster of Science and Engineering, Fukushima University, 1 Kanayagawa, Fukushima 960-1296, Japan; s1670001@ipc.fukushima-u.ac.jp

* Correspondence: daio@sss.fukushima-u.ac.jp; Tel.: +81-24-548-8199

Received: 20 July 2017; Accepted: 1 August 2017; Published: 3 August 2017

Abstract: A dicarbonylruthenium(II) complex containing bidentate 2-(2-pyridyl)-1,8-naphthyridine, as well as monodentate aqua and chlorido ligands, were isolated and characterized using spectroscopic techniques and single crystal X-ray diffraction. These data indicate that geometrical isomerization occurs during the substitution reaction involving a superacid. Density functional theory (DFT) calculations were performed on the plausible geometrical isomers. The DFT-optimized structures and calculated infrared spectra suggest that the experimentally obtained structure is stable.

Keywords: ruthenium complex; carbonyl; naphthyridine; X-ray diffraction; hydrogen-bonding; computational chemistry; vibrational spectroscopy

1. Introduction

Transition metal complexes containing carbonyl ligands have received considerable attention in the field of organometallic chemistry. In particular, carbonylruthenium(II) complexes with polypyridyl supporting ligands, such as 2,2'-bipyridine (bpy) or its derivatives, have proven to be active catalysts for the hydroformylation of olefins [1,2]. Additionally, 2-(2-pyridyl)-1,8-naphthyridine (pynp; Figure 1) is known to be a versatile ligand that functions not only as a bidentate polypyridyl ligand but also as an effective electron reservoir [3,4]. We recently reported the synthesis of carbonylruthenium(II) complexes containing both bpy and pynp [5]. As shown in Scheme 1, a synthetic strategy for sequential introduction of different bidentate ligands into ruthenium complexes was previously reported by both our group and Keene et al. [5,6]. These reports mentioned that treatment of the precursors with a superacid is the key step for both dissociation of the chlorido ligands and geometrical isomerization (i.e., the first step in Scheme 1). However, the reaction mechanism of the acid treatment has not yet been reported. To clarify when isomerization occurs, we isolated an intermediate in the acid-treatment reaction and determined its structure. Additionally, we explain the stability of the intermediate obtained using computational chemistry.

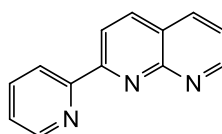
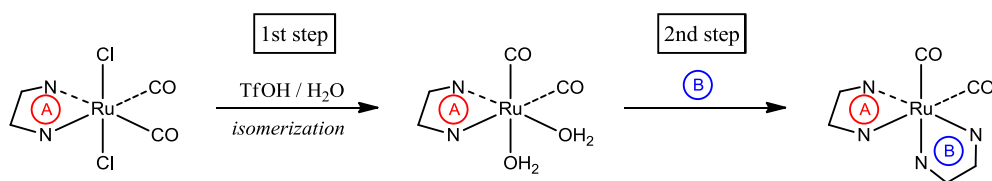


Figure 1. Chemical structure of pynp.



Scheme 1. A synthetic route for the introduction of different bidentate ligands [5]. (A) and (B) represent different bidentate ligands.

2. Results and Discussion

2.1. Isolation and Structure of the Title Compound

We performed acid treatment using *trans*-(Cl)-[Ru(pynp)(CO)₂Cl₂], which has been structurally analyzed [7], as the starting material. During the first step of Scheme 1, the reaction intermediate was promptly isolated. Spectroscopic measurements of the isolated compound (powder-compound) suggest that it is a mono-complex cation containing a mono-substituted ligand, i.e., [Ru(pynp)(CO)₂(OH₂)Cl]⁺. Additionally, the presence of two CO stretching vibrations in the infrared (IR) spectrum indicates that the two CO ligands are mutually coordinated in the *cis* position. Accordingly, there are five geometrical isomers (Figure 2). Since the molecular structure of the isolated complex could not be fully identified by spectroscopic measurements, the title compound was crystallized to perform single crystal X-ray diffraction. Although difficult, we successfully crystallized the compound (crystal-compound) by adding a small amount of bpy as a stabilizer. Among the structures shown in Figure 2, the formation of isomers (a) or (b) would be reasonable energetically (*vide infra*). It is expected that the aqua ligand in isomer (b) is quite chemically inert by an intramolecular hydrogen bonding between the non-coordinated nitrogen atom in pynp and the aqua moiety [8]. However, since the aqua ligand in both powder- and crystal-compounds is rapidly substituted by acetonitrile during measurement of mass spectra, we concluded that these are same structure (a). In addition, we confirmed that single crystals obtained consist of a single compound from spectral data of the crystal-compound.

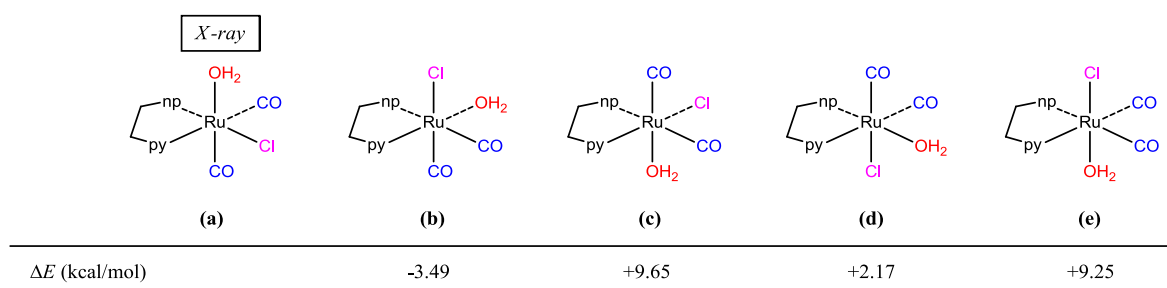


Figure 2. Possible geometrical isomers of *cis*(CO)-[Ru(pynp)(CO)₂(OH₂)Cl]⁺ with their electronic energy differences versus configuration (a). np and py denote 1,8-naphthyridyl and pyridyl rings, respectively.

As expected, this complex is a monocation from which one chlorido ligand is dissociated from the original complex (Figure 3). From the packing diagram, it is evident that the compound contains an additional bpy molecule in a 1:1 ratio (Figure 4). The geometrical structure of the cation corresponds to that shown in Figure 2a with Cl and OH₂ located in the *cis* position. Therefore, it was confirmed that the complex isomerized from *trans* to *cis* upon dissociation of one of the chlorido ligands.

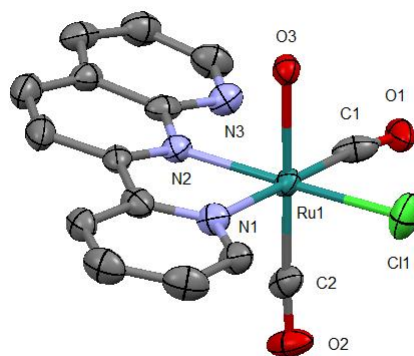


Figure 3. Molecular structure of the cation with atom labels and displacement ellipsoids for non-H atoms drawn at the 50% probability level. All H atoms are omitted for clarity.

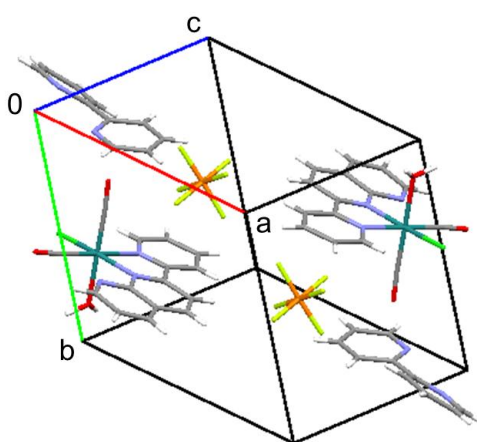


Figure 4. Packing diagram of the title compound.

In the obtained molecular structure, the substituted OH_2 ligand is coordinated *trans* to one of the CO ligands, the pyridine ring of pynp is coordinated *trans* to the other CO ligand, and the naphthyridine ring system of pynp is coordinated *trans* to the Cl ligand. The bond parameters of the Ru–CO Ru–Cl, and Ru–O moieties are comparable to those of similar ruthenium(II) complexes (Table 1) [7,9–11]. Of the two Ru–N bond lengths, the one involving the pyridine N atom is longer (2.128(4) vs. 2.074(4) Å) because of the *trans* effect of the carbonyl group. In addition, the interatomic distance between the CO carbon and non-coordinated N atoms in pynp ($\text{C1}\cdots\text{N3} = 2.687(6)$ Å) is considerably shorter than the sum of the van der Waals radii of C and N (3.25 Å); therefore, there is an electrostatic interaction between these atoms [12].

Table 1. Selected experimental and optimized bond parameters (Å, °) of $\text{cis}(\text{CO})\text{-}[\text{Ru}(\text{pynp})(\text{CO})_2(\text{OH}_2)\text{Cl}]^+$. The symbols (a to e) correspond to those in Figure 2.

Parameters	Expt.	(a)	(b)	(c)	(d)	(e)
<i>Bond lengths</i>						
Ru–O	2.114(3)	2.238	2.169	2.243	2.207	2.230
Ru–Cl	2.4002(12)	2.428	2.433	2.438	2.446	2.411
Ru–C1	1.860(5)	1.883	1.922	1.888	1.918	1.913
Ru–C2	1.910(5)	1.939	1.926	1.923	1.944	1.926
Ru–N _{py} ¹	2.128(4)	2.146	2.089	2.121	2.127	2.164

Table 1. Cont.

Parameters	Expt.	(a)	(b)	(c)	(d)	(e)
Ru–N _{np} ²	2.074(4)	2.139	2.173	2.172	2.095	2.160
C1–O1	1.134(6)	1.146	1.146	1.144	1.147	1.146
C2–O2	1.073(5)	1.143	1.143	1.144	1.143	1.144
<i>Bond angles</i>						
Ru–C1–O1	176.0(4)	178.7	179.3	179.9	179.7	177.4
Ru–C2–O2	171.6(5)	174.3	178.5	178.5	172.2	176.3

¹ N_{py} denotes the pyridyl nitrogen atom in pynp. ² N_{np} denotes the 1-naphthyridyl nitrogen atom in pynp.

In the crystal structure of the title compound, intermolecular hydrogen bonds exist between the aqua ligands and free bpy molecules (O···N distances: 2.713(6) and 2.742(5) Å; Figure 5). As a result of these interactions, the two pyridine rings in bpy show an unusual *cis*-conformation [13]. Therefore, these hydrogen bonds contribute to stabilization of the packing.

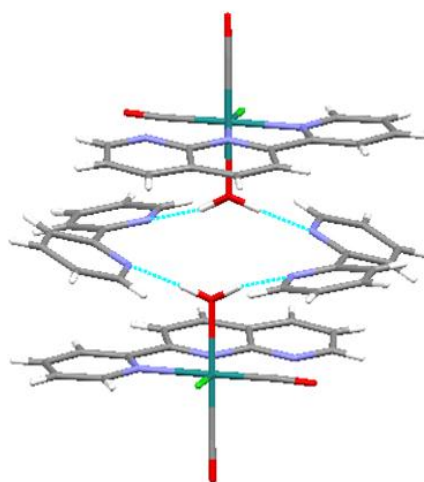


Figure 5. Intermolecular hydrogen bonds (blue dashed lines) in the crystal packing of the title compound.

DFT calculations were performed on the determined cation and other geometrical isomers in the gas phase; the optimized structure of (a) in Figure 2 shows good agreement with the experimental data (Table 1). Surprisingly, the most stable of these structures is (b) while (a) is the second most stable structure (energy difference: 3.5 kcal/mol). DFT calculations on a pair of the cation-bpy complexes, including four hydrogen bonds (Figure 5), revealed that the intermolecular interactions stabilized the complex by ~6 kcal/mol. Therefore, we concluded that the multiple intermolecular hydrogen bonds between the bpy nitrogen atoms and aqua ligands in (a) more significantly stabilize the crystal structure than the single intramolecular hydrogen bond between the non-coordinated nitrogen of pynp and aqua oxygen (2.681 Å) that is present in the theoretically most stable structure (Figure 2b).

2.2. Experimental and Calculated IR Spectra

Vibrational spectral data, such as stretching frequencies, often provide valuable information about the structure and bonding of carbonyl complexes; the ν_{CO} mode is particularly useful because it is generally free from coupling with other modes [14]. Therefore, the title compound was characterized by IR spectroscopy. Indeed, two very strong peaks were observed for the $\text{C}\equiv\text{O}$ stretching vibrations at 2095 and 2048 cm^{-1} (Figure S1); these values are in good agreement with those of terminal carbonyl ligands in analogous ruthenium(II) complexes [9].

To spectroscopically characterize the complex, we performed a frequency calculation analysis. The simulated IR data for νCO for the possible isomers and cation-bpy complex are given in Table S1. The calculations were performed on free molecules in a vacuum, while the experiments were performed on solid samples; therefore, the calculated and observed vibrational wavenumbers are expected to exhibit systematic differences. The CO stretching frequencies are similar values among possible isomers. It is difficult to distinguish configurations of the complex based on νCO data only.

3. Materials and Methods

3.1. General Methods and Physical Measurements

Electrospray ionization mass spectrometry (ESI-MS) data were obtained using a Bruker Daltonics micrOTOF (Bruker Daltonics, Yokohama, Japan). IR spectra were measured as KBr pellets using a JASCO FT-IR 4100 spectrometer (JASCO, Tokyo, Japan). A single crystal of $[\text{Ru}(\text{pynp})(\text{CO})_2(\text{OH}_2)\text{Cl}]\text{PF}_6 \cdot (\text{bpy})$ was analyzed on a Rigaku Saturn70 CCD diffractometer (Rigaku, Tokyo, Japan). The crystal was kept at 93 K during data collection. All calculations were conducted using *CrystalStructure* [15] except for refinement, which was performed using *SHELXL97* [16]. The non-hydrogen atoms were refined anisotropically. All H atoms bonded to C atoms were positioned geometrically and refined as a riding model. The H atoms in the aqua ligand were omitted from the structure.

3.2. Synthesis of $[\text{Ru}(\text{pynp})(\text{CO})_2(\text{OH}_2)\text{Cl}]\text{PF}_6$

All solvents for the synthesis were anhydrous and used without further purification. Ruthenium trichloride was purchased from Furuya Metal (Tokyo, Japan). Pynp and (OC-6-14)- $[\text{Ru}(\text{pynp})(\text{CO})_2\text{Cl}_2]$ were prepared according to previously reported procedures [7,17].

The procedure, which was inspired by a reported procedure [6], was applied to obtain the mono-substituted intermediate for X-ray measurement. $[\text{Ru}(\text{pynp})(\text{CO})_2\text{Cl}_2]$ (93 mg, 0.21 mmol) and trifluoromethanesulfonic acid (50%, 60 μL) were added to *o*-dichlorobenzene (30 mL). The mixture was refluxed for 90 min under N_2 . The reaction mixture was cooled and saturated methanolic NH_4PF_6 (1 mL) and diethyl ether (100 mL) were added to the solution, resulting in the formation of $[\text{Ru}(\text{pynp})(\text{CO})_2(\text{OH}_2)\text{Cl}]\text{PF}_6$ as a yellow precipitate. Single crystals suitable for X-ray diffraction analysis were obtained by vapor diffusion of diethyl ether into an acetone solution of the complex and a small amount of bpy over a few days.

$[\text{Ru}(\text{pynp})(\text{CO})_2(\text{OH}_2)\text{Cl}]\text{PF}_6 \cdot (\text{bpy})$. ESI-MS (CH_3CN): $m/z = 441.0$ ($[\text{M} - \text{OH}_2 + \text{CH}_3\text{CN}]^+$). IR (KBr): 2095, 2048 cm^{-1} (νCO), 839 cm^{-1} (νPF). Single crystal X-ray diffraction for $\text{C}_{25}\text{H}_{19}\text{ClF}_6\text{N}_5\text{O}_3\text{PRu}$ ($M_r = 718.94$): triclinic, space group $P\bar{1}$ (no. 2), $a = 10.0047(3)$, $b = 11.4277(3)$, $c = 13.1473(4)$ \AA , $\alpha = 66.5862(7)$, $\beta = 88.2422(7)$, $\gamma = 76.6993(7)^\circ$, $V = 1339.26(6)$ \AA^3 , $Z = 2$, $T = 93$ K, $\mu(\text{Mo } K\alpha) = 0.826$ mm^{-1} , $D_{\text{calc}} = 1.783$ g/cm^3 , 14008 reflections measured, 6045 unique ($R_{\text{int}} = 0.0355$), which were used in all calculations. The final R_1 was 0.0493 ($I > 2\sigma(I)$) and wR_2 was 0.1202 (all data). CCDC 1561540 contains the supplementary crystallographic data for this paper. These data can be obtained free of charge via <http://www.ccdc.cam.ac.uk/conts/retrieving.html>.

3.3. Computational Details

DFT calculations were performed on (a) to (e) (in Figure 2) and the cation-bpy complex. The ground-state, gas-phase structures of these compounds were optimized at the DFT level (B3LYP) [18,19]. The LanL2DZ basis set was employed for the ruthenium atoms [20], and the 6-31 G(d) basis set was employed for the other atoms [21,22]. The harmonic vibrational frequencies were calculated at the same levels of theory for the optimized structures and no imaginary frequencies were found. All calculations were performed using the Gaussian 09W program package [23].

Supplementary Materials: The following are available online at www.mdpi.com/1422-8599/2017/3/M950. Figure S1: IR spectrum of the title compound (KBr pellet) and Table S1: Comparison between the experimental and DFT-calculated IR peaks for ν_{CO} .

Acknowledgments: This work was supported by JSPS KAKENHI, Grant Number: JP17K05799 (JSPS, Japan).

Author Contributions: D.O. conceived and designed the experiments; R.A. and T.T. performed the experiments; T.T. performed the calculations; T.T. and D.O. co-wrote the manuscript.

Conflicts of Interest: The authors declare no conflict of interest.

Appendix Appendix

Although the configurations in Figure 2 have both *C* and *A* enantiomers, only the *A*-isomers are presented [24].

References

1. Mitsudo, T.; Suzuki, N.; Kondo, T.; Watanabe, Y. Ru₃(CO)₁₂/1,10-phenanthroline-catalyzed hydroformylation of α -olefins. *J. Mol. Catal. A*. **1996**, *109*, 219–225. [CrossRef]
2. Moya, S.A.; Gajardo, J.; Araya, J.C.; Cornejo, J.J.; Guerchais, V.; Le Bozec, H.; Bayón, J.C.; Pardey, A.J.; Aguirre, P. Synthesis and characterization of new complexes of the type [Ru(CO)₂Cl₂(2-phenyl-1,8-naphthyridine- κ N)(2-phenyl-1,8-naphthyridine- κ N')]. Preliminary applications in homogeneous catalysis. *Appl. Organometal. Chem.* **2008**, *22*, 471–478. [CrossRef]
3. Oyama, D.; Hamada, T.; Takase, T. Stereospecific synthesis and redox properties of ruthenium(II) carbonyl complexes bearing a redox-active 1,8-naphthyridine unit. *J. Organomet. Chem.* **2011**, *696*, 2263–2268. [CrossRef]
4. Oyama, D.; Yuzuriya, K.; Naoi, R.; Hamada, T.; Takase, T. Syntheses of geometrical isomers for comparison of properties caused by steric and electronic effects in carbonylruthenium(II) complexes. *Bull. Chem. Soc. Jpn.* **2014**, *87*, 1107–1115. [CrossRef]
5. Oyama, D.; Abe, R.; Takase, T. CO-ligand photodissociation in two Ru(II) complexes affected by different polypyridyl supporting ligands. *Chem. Lett.* in press [CrossRef]
6. Anderson, P.A.; Deacon, G.B.; Haarmann, K.H.; Keene, F.R.; Meyer, T.J.; Reitsma, D.A.; Skelton, B.W.; Strouse, G.F.; Thomas, N.C.; Treadway, J.A.; et al. Designed synthesis of mononuclear tris(heteroleptic) ruthenium complexes containing bidentate polypyridyl ligands. *Inorg. Chem.* **1995**, *34*, 6145–6157. [CrossRef]
7. Oyama, D.; Hamada, T. *cis,trans*-Dicarbonyldichlorido[2-(2-pyridyl)-1,8-naphthyridine- κ N¹,N²]ruthenium(II). *Acta Cryst.* **2008**, *E64*, m442–m443. [CrossRef] [PubMed]
8. Oyama, D.; Yamanaka, T.; Fukuda, A.; Takase, T. Modulation of intramolecular hydrogen-bonding strength by axial ligands in ruthenium(II) complexes. *Chem. Lett.* **2013**, *42*, 1554–1555. [CrossRef]
9. Oyama, D.; Asuma, A.; Hamada, T.; Takase, T. Novel [Ru(polypyridine)(CO)₂Cl₂] and [Ru(polypyridine)₂(CO)Cl]⁺-type complexes: Characterizing the effects of introducing azopyridyl ligands by electrochemical, spectroscopic and crystallographic measurements. *Inorg. Chim. Acta* **2009**, *362*, 2581–2588. [CrossRef]
10. Oyama, D.; Suzuki, K.; Yamanaka, T.; Takase, T. One-pot synthesis of *cis*-bis(2,2'-bipyridine) carbonylruthenium(II) complexes from a carbonato precursor: X-ray crystal structures and electron transfer processes of the series complexes. *J. Coord. Chem.* **2012**, *65*, 78–86. [CrossRef]
11. Takase, T.; Takahashi, K.; Oyama, D. *cis,trans*-Dicarbonyldichlorido(1,10-phenanthroline-5,6-dione- κ^2 N,N') ruthenium(II). *IUCrData* **2017**, *2*, x170288. [CrossRef]
12. Oyama, D.; Ukawa, N.; Hamada, T.; Takase, T. Reversible intramolecular cyclization in ruthenium complexes induced by ligand-centered one-electron transfer on bidentate naphthyridine: An important intermediate for both metal- and organo-hydride species. *Chem. Lett.* **2015**, *44*, 533–535. [CrossRef]
13. Abe, R.; Takase, T.; Oyama, D. 2-(Pyridin-2-yl) pyridinium trifluoromethanesulfonate. *IUCrData* **2017**, *2*, x170689. [CrossRef]
14. Nakamoto, K. *Infrared and Raman Spectra of Inorganic and Coordination Compounds*, 4th ed.; John Wiley & Sons: New York, NY, USA, 1986; pp. 291–308.
15. Rigaku. *CrystalStructure*; Version 4.0; Rigaku Corporation: Tokyo, Japan, 2010.
16. Sheldrick, G. A short history of SHELX. *Acta Cryst.* **2008**, *A64*, 112–122. [CrossRef] [PubMed]

17. Campos-Fernández, C.S.; Thomson, L.M.; Galán-Mascarós, J.R.; Ouyang, X.; Dunbar, K.R. Homologous series of redox-active, dinuclear cations $[M_2(O_2CCH_3)_2(pynp)_2]^{2+}$ (M = Mo, Ru, Rh) with the bridging ligand 2-(2-pyridyl)-1,8-naphthyridine (pynp). *Inorg. Chem.* **2002**, *41*, 1523–1533. [[CrossRef](#)] [[PubMed](#)]
18. Becke, A.D. Density-functional thermochemistry. III. The role of exact exchange. *J. Chem. Phys.* **1993**, *98*, 5648–5652. [[CrossRef](#)]
19. Lee, C.; Yang, W.; Parr, R.G. Development of the Colle-Salvetti correlation-energy formula into a functional of the electron density. *Phys. Rev. B* **1988**, *37*, 785–789. [[CrossRef](#)]
20. Hay, P.J.; Wadt, W.R. Ab initio effective core potentials for molecular calculations. Potentials for the transition metal atoms Sc to Hg. *J. Chem. Phys.* **1985**, *82*, 270–283. [[CrossRef](#)]
21. Hehre, W.J.; Ditchfield, R.; Pople, J.A. Self-consistent molecular orbital methods. XII. Further extensions of Gaussian-type basis sets for use in molecular orbital studies of organic molecules. *J. Chem. Phys.* **1972**, *56*, 2257–2261. [[CrossRef](#)]
22. Francl, M.M.; Pietro, W.J.; Hehre, W.J.; Binkley, J.S.; Gordon, M.S.; DeFrees, D.J.; Pople, J.A. Self-consistent molecular orbital methods. XXIII. A polarization-type basis set for second-row elements. *J. Chem. Phys.* **1982**, *77*, 3654–3665. [[CrossRef](#)]
23. Frisch, M.J.; Trucks, G.W.; Schlegel, H.B.; Scuseria, G.E.; Robb, M.A.; Cheeseman, J.R.; Scalmani, G.; Barone, V.; Mennucci, B.; Petersson, G.A.; et al. *Gaussian 09W*; Revision D.01; Gaussian, Inc.: Wallingford, CT, USA, 2009.
24. Connelly, N.G.; Damhus, T.; Hartshorn, R.M.; Hutton, A.T. *Nomenclature of Inorganic Chemistry, IUPAC Recommendations 2005*; Royal Society of Chemistry: Cambridge, UK, 2005.



© 2017 by the authors. Licensee MDPI, Basel, Switzerland. This article is an open access article distributed under the terms and conditions of the Creative Commons Attribution (CC BY) license (<http://creativecommons.org/licenses/by/4.0/>).